JOURNAL OF GEOPHYSICAL RESEARCH, VOL. 111, B12404, doi:10.1029/2005JB003879, 2006

Tectonic stress and magma chamber size as controls on dike propagation: Constraints from the 1975–1984 Krafla rifting episode

W. Roger Buck,[1] Páll Einarsson,[2] and Bryndís Brandsdóttir[2]

Received 9 June 2005; revised 27 April 2006; accepted 30 June 2006; published 9 December 2006.

[1] The best-studied dike intrusion events on a divergent plate boundary occurred along the Krafla segment of the northern rift zone in Iceland from 1975–1984. Seismic and geodetic measurements there showed that a central magma chamber fed dikes that propagated laterally many times the thickness of the lithosphere. The patterns of dike length, dike width, caldera subsidence, and lava extrusion strongly suggest that dike propagation is affected by tectonic stresses that change with each dike intrusion event and that magma pressures are linked to the dike opening. These observations have inspired us to develop a quantitative model for the lateral propagation of basaltic dikes away from a magma chamber. We assume dikes propagate as long as there is sufficient driving pressure, defined as the difference between magma pressure and tectonic stress at the dike tip. The opening dike and the magma chamber are treated as a closed system for a given dike intrusion event. During an event, magma pressure is reduced linearly with the magma volume withdrawn from the chamber. Relative tectonic tension in the lithosphere is reduced linearly as the dike width increases. A dike begins propagation when the driving pressure equals the ''breakout'' pressure needed to force the magma out of the chamber. It stops when the driving pressure reaches a minimum value. Generally, the dike width is proportional to this ''stopping'' pressure, and a reasonable value gives a width of 1 m. Besides the breakout and stopping pressures, the propagation distance depends on the initial distribution of tectonic stress and the thickness of the lithosphere cut by a dike. The intrusion of a dike changes the tectonic stress distribution so that subsequent dikes may propagate different distances and directions than the first dike. After a period of magma chamber refilling, a new dike can initiate if the breakout pressure is reached. For an idealized spreading segment the tectonic stress field evolves to produce a sequence of dikes propagating in one direction followed by a sequence of dikes propagating in the opposite direction. The first dike in each sequence should be the longest followed by successively shorter dikes. When tectonic stresses close to a magma chamber have been largely relieved, then extrusion of magma may start. The model pattern of dike propagation and extrusion is consistent with data from the Krafla episode. Magma chamber size should have a major effect on magmatic systems in other tectonic settings with larger magma chambers producing longer characteristic dikes.

Citation: Buck, W. R., P. Einarsson, and B. Brandsdóttir (2006), Tectonic stress and magma chamber size as controls on dike propagation: Constraints from the 1975–1984 Krafla rifting episode, *J. Geophys. Res.*, *111*, B12404, doi:10.1029/2005JB003879.

1. Introduction

[2] Dike intrusion is the quantum event of crustal accretion at divergent plate boundaries such as oceanic spreading centers and continental rifts [e.g., *Delaney et al.*, 1998]. Dikes appear to accommodate most of the separation of tectonic plates at mid-ocean ridges and seismic layer 2b of oceanic crust is thought to be composed mainly of dikes [*MacDonald*, 1998]. Studies of ophiolites and tectonic exposures of oceanic crust show sheeted dike units composed of thousands of ~meter thick dikes [*Karson*, 1998]. The breakup of large continents by rifting is nearly always accompanied by copious magmatism and related dike intrusion on distance scales of thousands of kilometers [e.g., *White and McKenzie*, 1989]. However, there is no consensus on what controls how far dikes propagate and how often dikes form at ridges and in rifts.

[3] The most obvious way to learn about how spreading center dikes work is to observe and analyze active intrusion events. Despite vigorous efforts to gather data on diking at

[1] Lamont-Doherty Earth Observatory, Columbia University, Palisades, New York, USA.
[2] Institute of Earth Sciences, University of Iceland, Reykjavík, Iceland.

0148-0227/06/2005JB003879$09.00

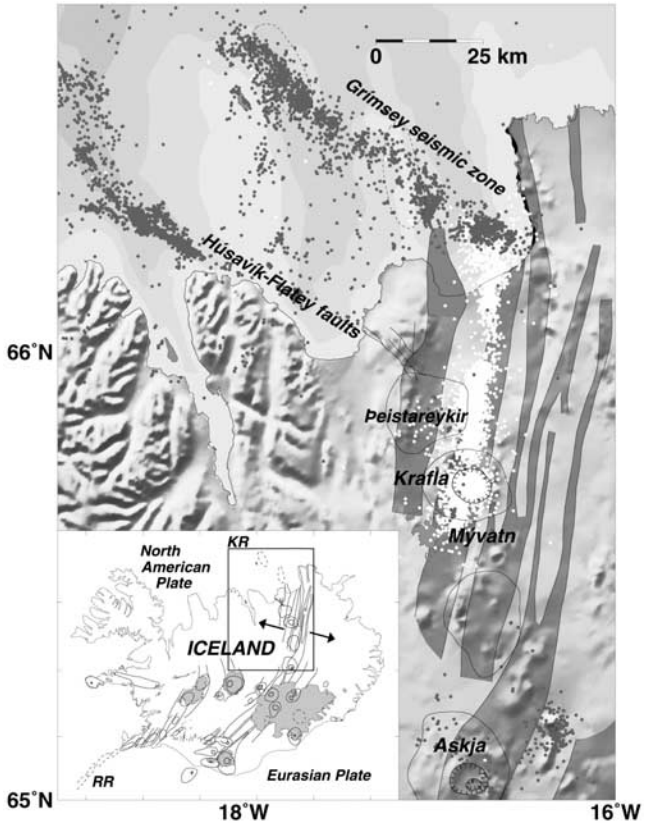

Figure 1. Map showing location of volcanic systems along the plate boundary in Iceland. The systems active in the last centuries in North Iceland, the Theistareykir, Krafla, and Askja systems have an en echelon arrangement and overlap to a considerable degree. The main branches of the Tjörnes Fracture Zone, the Grímsey seismic zone, and the Húsavík-Flatey faults are delineated by epicenters of 1995–2003 (black dots), provided by the Icelandic Meteorological Office. White dots are epicenters of events during the Krafla rifting episode. Fissure swarms (dark stripes), central volcanoes (shown by thin, closed lines), and calderas are taken from *Einarsson and Saemundsson* [1987].

divergent plate boundaries there are only a few observations available. Monitoring seismicity on the submarine Juan de Fuca Ridge allowed rapid response teams to observe effects of dike intrusion events such as the expulsion of biological material from the crust into the water [e.g., *Embley et al.*, 1995; *Dziak et al.*, 1995]. A more comprehensive data set collected during a period of earthquake and magmatic activity called the Krafla magmatic-tectonic episode that took place along the northern rift zone in Iceland from 1974 to 1989 [e.g., *Björnsson et al.*, 1977; *Einarsson*, 1991]. The Krafla rifting episode consisted of a total of about 20 diking events that occurred between 1975 and 1984.

[4] Most dike model studies focus on individual dikes while the emphasis of this paper is treating changes in tectonic stress during a sequence of dikes in an episode. In this paper we describe key features of the Krafla dike intrusion events, which were carefully studied with seismic and geodetic methods. Next, we describe the formulation of a simple model for dike propagation linking tectonic stress and magma pressure. We show that a few physical parameters can describe a fairly complex pattern of dike propagation distance, dike widening and caldera deflation similar to what was observed during the Krafla episode. Finally, we suggest ways this model may be applied to other areas where parameters such as lithospheric thickness are known to be different.

2. Krafla Rifting Episode

[5] A sequence of discrete rifting events occurred along the plate boundary in North Iceland, beginning in 1975 and lasting until 1984. It was accompanied by the largest earthquake sequence so far recorded along the divergent plate boundaries of the Atlantic [*Einarsson*, 1986]. The events took place mainly within the Krafla volcanic system between latitudes of 65°34′N and 66°18′N (Figure 1) that is one of several systems constituting the boundary between the European and North American lithosphere plates in North Iceland [*Saemundsson*, 1974, 1979]. The volcanic system consists of a central volcano with associated fissure swarms that extend along the plate boundary perpendicular to the plate separation vector. By fissure swarm we mean a spatially clustered set of subparallel fissures and normal faults.

[6] A localized magma chamber has been identified within the caldera of the volcano, both by seismic methods [*Einarsson*, 1978; *Brandsdóttir et al.*, 1997] and geodetic location of a source of variable pressure [e.g., *Tryggvason*, 1980; *Ewart et al.*, 1991]. During most of the episode, magma apparently ascended from depth and accumulated in the magma chamber at about 3 km depth. The inflation periods were punctuated by sudden deflation events lasting from several hours to 3 months when the walls of the chamber were breeched and magma was injected laterally into the adjacent fissure swarm where subsequently large-scale rifting took place (Figure 2). During each event the

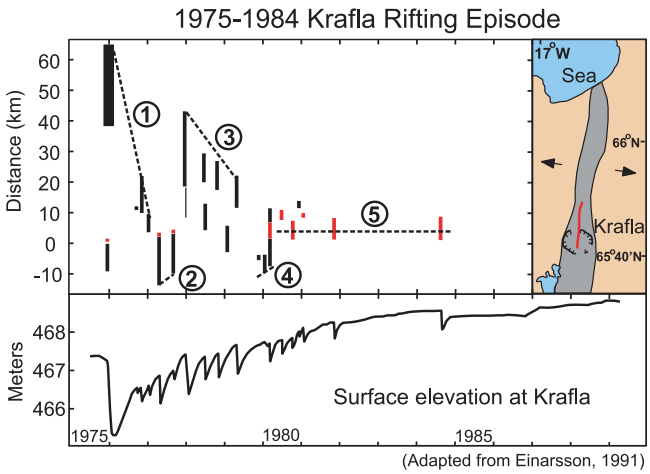

Figure 2. Observations with time during the Krafla episode 1974–1989. (top) Distance ranges for surface fissuring (black) or extrusion of lava (red) measured from the center of the Krafla inflation (shown on the map, right). The thickness of the vertical lines gives the time duration of the activity. (bottom) Changes in the elevation near the center of inflation in the Krafla caldera. Tick marks are for the beginning of each year. From *Einarsson* [1991], reprinted by permission.

flanks of a segment of the fissure swarm moved away from each other.

[7] A total of about 20 discrete rifting events were identified, each one affecting only a portion of the fissure system [*Björnsson et al.*, 1979; *Tryggvason*, 1980; *Einarsson*, 1991]. The rifting events were observed to open new and old surface fissures, and to cause vertical displacements on several faults [*Sigurdsson*, 1980]. Most of the fissure movements occurred along a 1 to 2 km wide zone within the 4 to 8 km wide Krafla fissure swarm. Subsidence within the Krafla caldera was concurrent with rifting and widening of segments of the Krafla fissure swarm [*Björnsson et al.*, 1977, 1979; *Tryggvason*, 1980, 1984, 1994]. Studies of the seismicity associated with each event are consistent with dikes that propagate at a 1 to 2 m/s rate from a central magma source [*Brandsdóttir and Einarsson*, 1979; *Einarsson and Brandsdóttir*, 1980]. The seismicity shows activity as deep as 10 km below the surface. Early events in the episode produced as much as 2 m slip on normal faults [*Björnsson et al.*, 1977; *Tryggvason*, 1984] and little or no lava extrusion. During some eruption events the lava flowed back into the uppermost crust via surface fissures [*Einarsson*, 1991]. Primary extrusion of lavas was mainly confined to the last few events in the sequence [*Tryggvason*, 1994], when the dikes reached the surface in fissure eruptions lasting from 5 to 14 days.

[8] The sequence of events shows remarkable regularities (Figure 2). Subsequences may be identified within the magmatic episode, each of them consisting of dikes of decreasing length.

[9] Subsequence 1. The initial event began on 20 December 1975 with a small eruption at the center of inflation within the Krafla caldera, accompanied by rapid deflation, rifting and lateral magma injection into the adjacent fissure swarm, first to the south and then to the north. This event followed a period of over a year of elevated earthquake activity in the caldera. The largest amount of rifting occurred at the northern end of the fissure swarm, near its intersection with the Grímsey oblique rift, triggering a magnitude 6.5 (M_S) strike-slip earthquake within that zone on 13 January. The deflation lasted until the middle of March 1976 when inflation resumed within the Krafla caldera. The next event lasted from 29 September to 4 October 1976. No surface rifting was identified but small earthquakes were located 12 km north of the caldera. More dramatic events occurred on 31 October 1976 and 20 January 1977 when large-scale rifting was witnessed 10–24 km and 5–10 km north of the caldera, respectively.

[10] Subsequence 2. Two events followed in the southern fissure swarm, beginning on 27 April and 8 September 1977. Both events began with small eruptions near the northern caldera rim that quickly ended when earthquakes propagated to the south. The April event was accompanied by continuous rifting from the center of inflation within the caldera and 13 km to the south, the September event similarly up to 10 km south of the caldera. A small amount of basaltic pumice was ejected from a geothermal borehole in the southern fissure swarm during the rifting on 8 September [*Larsen et al.*, 1979]. A third, very small event on 2 November 1977, was probably associated with diking within the caldera.

[11] Subsequence 3. This sequence consisted of four large rifting events in the fissure swarm north of the caldera, beginning on 8 January, 10 July, and 10 November 1978, and 13 May 1979. Rifting during these events was concentrated 20–45 km, 5–30 km, 16–28 km and 12–24 km north of the caldera, respectively.

[12] Subsequence 4. Three deflation events in 1979–1980 were associated with earthquakes and rifting in the fissure swarm south of the caldera. A small event in December 1979 was associated with small earthquakes, most likely slightly south of the caldera, but no fissures were found at the surface. A relatively small event began on 10 February, accompanied by earthquakes at 7–9 km depth, 0–10 km south of the caldera, almost in the same section as the September event of 1977 but at slightly greater depth. A rapid deflation event on 17 March 1980 resulted in a small eruption on a 6 km long and intermittent fissure extending from the center of the caldera northward. The eruption stopped when rifting began, propagating from the caldera into the southern fissure swarm.

[13] Subsequence 5. The Krafla rifting episode ended with a sequence of fissure eruptions, each of which was associated with deflation of the caldera region and began in the same fashion as the rifting events had done previously. All these eruptions took place within in the same section of the fissure swarm, extending from the center of the caldera and about 9 km to the north. They occurred on 10–18 July 1980 (30 Mm^3), 18–23 October 1980 (40 Mm^3), 30 January to 4 February 1981 (40 Mm^3), 18–23 November 1981 ($\sim$40 Mm^3), and 4–18 September 1984 ($\sim$80 Mm^3). One small noneruptive deflation event happened between the eruptions, in December 1980. This was a slow event, with a flurry of small earthquakes just north of the caldera.

[14] Following the last eruption, the Krafla magma chamber inflated again until the preeruption level was approached. Then the inflation became intermittent. The last inflation period occurred in the summer of 1989. Since then the caldera region has been slowly subsiding [*Sigmundsson et al.*, 1997], a few centimeters per year. A total of $\sim$250 Mm^3 of basaltic lava were erupted during the Krafla episode but a substantially larger volume was emplaced in the crust [*Tryggvason*, 1994].

[15] Frequent distance measurements across the Krafla fissure swarm were conducted in order to monitor the extension accompanying the sequence of rifting events (Figures 3 and 4). Maximum widening of about 9 m occurred 10 to 12 km north of the center of inflation of the Krafla magma reservoir [*Tryggvason*, 1994]. From that location the amount of widening decreased northward and is estimated at between 2 and 5 m where the seismicity indicated the northern termination of the present rifting, off the north coast, about 70 km north of the inflation center. The amount of widening also decreased southward and approached zero at 15 to 20 km south of the inflation center [*Tryggvason*, 1984, 1994].

[16] Rifting episodes of the Krafla 1975–1984 type appear to take place in the northern rift zone of Iceland about every 100–150 years [*Björnsson et al.*, 1977; *Gudmundsson*, 1995], and the eastern rift in South Iceland seems to have comparable frequency [*Larsen*, 1984]. The most recent episodes in the northern rift zone are the Theistareykir events in 1618, the Krafla episode of 1724–

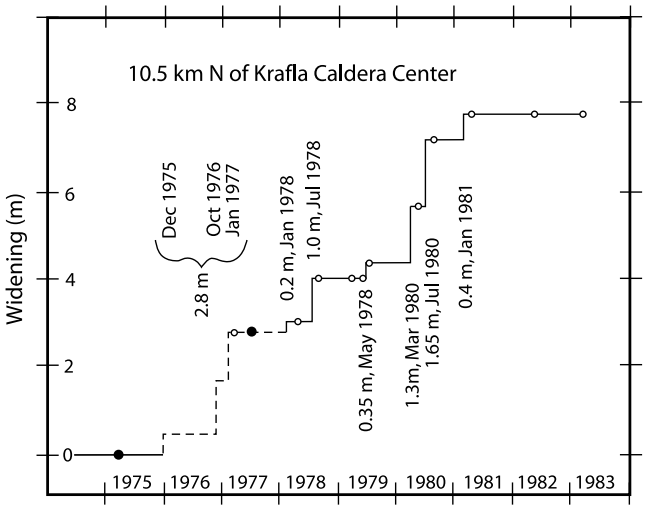

Figure 3. Observed horizontal opening with time in the fissure swarm ~10 km north of the center of inflation in the Krafla caldera. Comparison with data in Figure 2 indicates no correlation between the width of the dike-induced opening and the distance of dike propagation. From *Tryggvason* [1984], with kind permission of Springer Science and Business Media.

1729 (Myvatnseldar), and the Askja episode of 1874–1875. The Theistareykir events involved earthquakes and fissuring, but no lava extrusion. The other episodes were characterised by earthquakes and fissuring in the beginning, followed by lava extrusion. During the early stages of the Krafla 1975–1984 activity these previous episodes served as an important basis for forecasts of likely scenarios. It was a generally accepted view that the activity would become more eruptive toward the later stages [*Einarsson*, 1991] when the extensional stress across the plate boundary would be relieved by the rifting activity.

[17] The Krafla data imply that the evolution of a tectonic stress field could affect dike intrusions and this is a major component of the model described in this paper. The other key model component inspired by these data is that magma intruding a dike is supplied by a central magma chamber and that dike opening reduces magma chamber pressure. A link between magma chamber pressure and dike opening is also inferred for Kilauea Volcano [*Segall et al.*, 2001]. *Takada* [1997] agrees that evolution of tectonic stress may produce the kind of pattern of dike lengths with time seen at Krafla and he further shows that several other basaltic volcanoes show similar patterns of alternating directions of dike propagation sequences with diminishing lengths of propagation. The qualitative model suggested by *Takada* [1997] is much like the quantitative model we describe in this paper. Before we formulate that model, we briefly review other ideas about processes that may affect dike propagation.

3. Previous Models for Dike Propagation

[18] Dikes are essentially fluid filled cracks and their propagation may be controlled by a dauntingly large number of thermal and mechanical processes. Among them are the pressure and flux of magma coming out of a source region, the viscous resistance to magma flow along the body of the dike and into the tip region, elastic stresses in lithosphere and the freezing of magma [e.g., *Lister and Kerr*, 1991; *Rubin*, 1995]. Any model for dike propagation has to ignore or simplify some of the processes that plausibly could affect dike intrusion.

[19] The model most often discussed for dike propagation, the thermal entrance length model [e.g., *Delaney and Pollard*, 1982; *Rubin*, 1993; *Lister*, 1994; *Fialko and Rubin*, 1998], ignores complications of the source and tip region. This model considers an "open system" in which controlling parameters, the magma pressure and the dike width, are imposed from outside the model domain. Resistance to viscous flow of magma in the body of the dike limits the rate of flow of magma. The magma cools as it flows along the body of the dike and at a certain dike length the magma reaching the dike tip begins to freeze, thus limiting dike propagation. The distance a dike can propagate into cold rock before freezing up, the thermal entrance length, depends strongly on the dike width: wide dikes go much farther than narrow dikes. There is some evidence from the eroded remains of ancient dike complexes that wide dikes may propagate larger distances than do smaller dikes [see *Fialko and Rubin*, 1999]. Unfortunately, the model provides no insight into what controls the dike width.

[20] Observations from the Krafla episode do not support the prediction that dike width is the main control on distance of dike propagation. Geodetic data indicates nearly the same widening of the fissure swarm in each event, while the propagation distance varied greatly [e.g., *Tryggvason*, 1984] (Figures 2, 3, and 4). Also, the first dike in the Krafla sequence indicates that freezing did not stop its propagation.

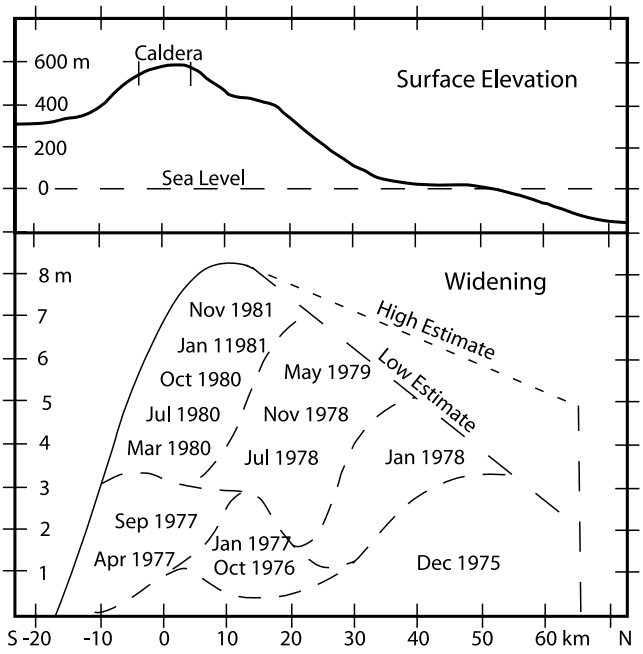

Figure 4. Estimated total opening of the fissure swarm versus distance from the inflation center during the events of the Krafla episode from *Tryggvason* [1984]. Note that the 1984 event was not included in this figure and adds about 1 m of opening close to the caldera.

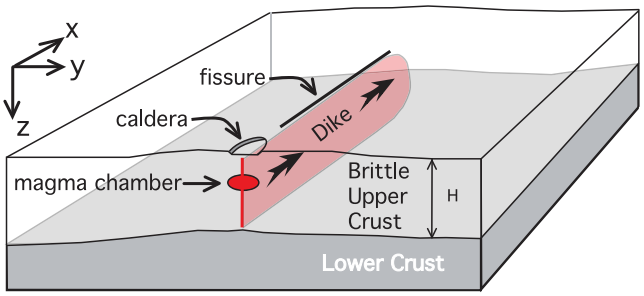

Figure 5. Block diagram illustrating the geometry of a dike fed by a magma chamber. The x value is the horizontal distance from the chamber along the dike and z is depth below the surface at the origin. Fissures may open above a dike in some cases of dike emplacement.

That dike took 2 days to reach a transform fault system 70 km north of the caldera where it stopped propagating, but it continued to open and drain the magma chamber for ~3 months. It is plausible that a stress barrier stopped this dike and a connection between the magma chamber and the dike remained open for months.

[21] The lack of fast magma freezing may be due to the depth of dike opening. We expect that dikes propagating laterally farther than a lithospheric thickness should cut through the entire lithosphere and possibly into the hot, weak asthenosphere (Figures 5 and 6). The time to cool magma in a dike is proportional to the inverse square of the temperature contrast between magma and host rock [*Turcotte and Schubert*, 2002]. As long as the host rock is colder than about 600°C then basaltic dikes should freeze on the observed timescale of propagation [*Fialko and Rubin*, 1998]. However, temperatures at the base of the lithosphere are likely to be more than 1000°C [*Hirth et al.*, 1998]. Magma flowing through the hot lower lithosphere could continue to supply meter wide dikes for times much longer than the observed propagation times. Lateral flow of hot magma could even lead to ablative widening of the dike at the base of the lithosphere [*Bruce and Huppert*, 1990], perhaps allowing an open "pipe" from the magma chamber to a dike even when the dike near the magma chamber has

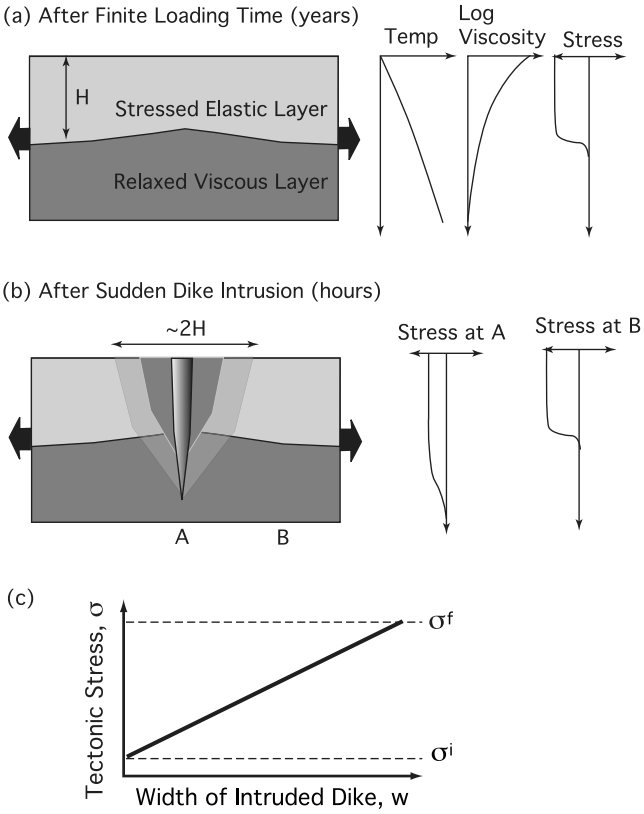

Figure 6. Illustration of stress changes in a representative cross section of along-axis lithosphere and asthenosphere. (a) Cold, high-viscosity lithosphere maintaining a stress difference (the difference between horizontal and lithostatic stress) due to plate separation. The hotter asthenosphere has such a low viscosity that on the timescale of plate separation no significant stress differences are maintained. (b) Stresses change immediately after intrusion of a dike. Stress differences are relieved in the lithosphere in the region close to the dike (indicated by the shading that does not extend out to B), but the asthenosphere is extensionally stressed near the axis of dike intrusion.

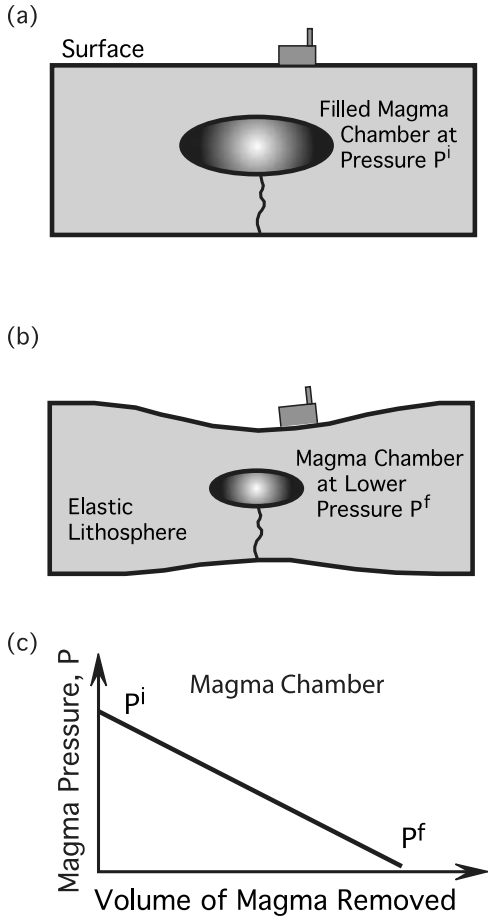

Figure 7. Illustration of the effect of magma chamber deflation. (a) Filled magma chamber and reference ground surface. (b) Removal of magma from the chamber results in a reduction of pressure in the chamber and a drawdown of the surface. (c) Plot of linear decrease in chamber pressure with the volume of magma withdrawn.

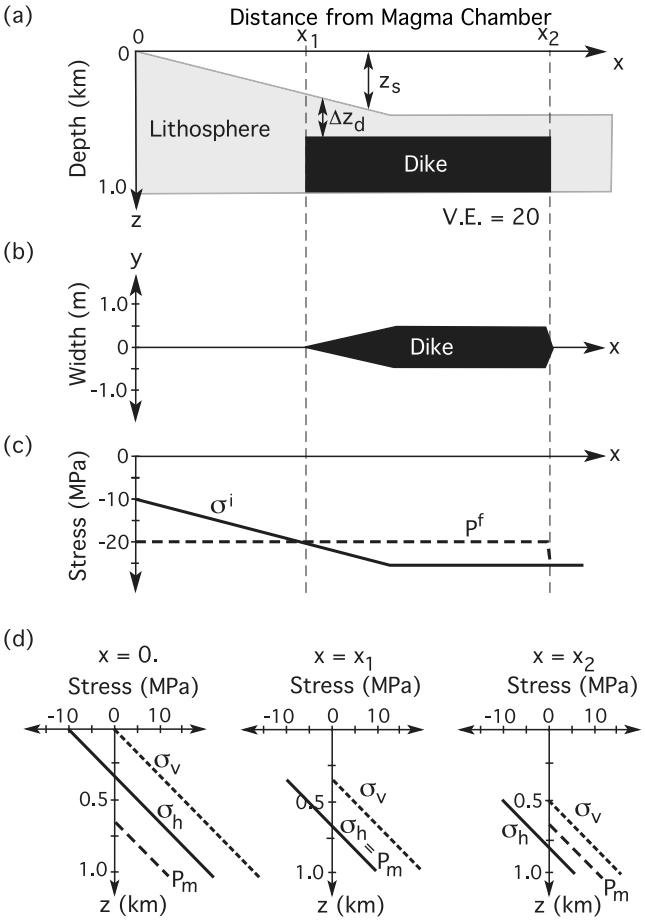

Figure 8. Geometry of idealized dike intrusion and associated stresses. (a) Variation of lithospheric surface depth z_s with distance x referenced to the surface at the magma chamber source at $x = 0$. Depth Δz_d of dike below the local lithospheric surface. (b) Width of dike as a function of x, where x_1 and x_2 are the ends of the dike closest and farthest from the origin, respectively. (c) Horizontal variation in the initial tectonic stress and final magma pressure (defined in text) which control the dike opening. (d) Vertical variation of lithospheric stress and magma pressure with depth for the three horizontal positions indicated. Here the magma and lithospheric densities equal 3000 kg/m^3, and the acceleration of gravity is 10 m/s^2.

closed. For example the first dike in the Krafla episode continued to open >30 km from the caldera while opening did not continue closer to the caldera.

[22] Another feature of the Krafla events suggests that viscous flow related pressure gradients might not be as important as the thermal entrance model assumes. Most dikes began propagating with velocities around 2 m/s and gradually slowed before stopping [*Einarsson and Brandsdóttir*, 1980]. During propagation the Krafla caldera subsided steadily, but deflation ceased within seconds of the time the dikes stopped propagating, as indicated by a marked reduction in seismicity [*Einarsson*, 1991]. This indicates that dike widening stopped when the tip stopped opening. If there were sizable dynamic pressure reductions along the dike when it stopped propagating then we would expect parts of the dike to continue widening, and so magma would be pulled out of the chamber, as pressures relaxed toward static values. The ablative widening of the deeper parts of the dike, discussed above, could greatly reduce the pressure gradient required to drive lateral magma flow.

[23] A recent dike propagation model by *Ida* [1999] ignores freezing of magma and considers that driving pressures control the distance of dike propagation. Ida assumes that magma pressure decreases linearly with the volume of magma withdrawn from the chamber as we do (see Figure 7). This model treats the dike as a semiinfinite crack to calculate the resistance to tip opening according to a fracture toughness criteria. For horizontal dike propagation this implies the dike is infinitely tall and far from the dike tip the dike opening does not change tectonic stresses. Because of this approximation, *Ida* [1999] comes to the conclusion that larger tectonic relative tension leads to shorter dikes. This is opposite to what appears to happen for Krafla, where early dikes in a subsequence travel the farthest. The critical difference between our model and Ida's model is that we assume dike opening is resisted along the entire length dike and at the tip, while Ida only deals with resistance at the tip.

4. Model Formulation: Linked Tectonic Stress and Magma Pressure

[24] We would like to relate the evolution of properties of a tectonic-magmatic system, such as stresses in the lithosphere, to observable features, such as the distance range of dike opening during magmatic intrusion events. To do this in a simple way we neglect magma cooling and viscous pressure changes along the body of the dike. A basic assumption is that dike propagation is driven by the difference between magma pressure, P_m, and the minimum principal stress in the lithosphere, σ_H, which is directed normal to the plane of a vertical dike. Both of these quantities can vary with depth, z, but only the stress is taken to vary with horizontal distance from the magma chamber along the dike, x (Figure 8; see also the Notation section).

4.1. Conventions and Definitions

[25] We follow the geologic convention that compressive stress is positive and that principal stresses are either vertical or horizontal. The magma pressure is assumed to be the static pressure and so varies only with the vertical hydrostatic gradient. Then the depth-dependent magma pressure can be described as

$$P_m(z) = P + \rho g z, \tag{1}$$

where P is the pressure at the surface above the magma chamber at $x = 0$, ρ is the magma density, and g is the acceleration of gravity. The surface at $x = 0$ is taken to be at a depth $z = 0$.

[26] The vertical stress is taken to be the lithostatic stress and is given by

$$\sigma_v(x, z) = \rho g(z - z_s(x)), \tag{2}$$

where ρ is the density of the lithosphere and $z_s(x)$ is the depth of the surface relative to the depth of the surface over

the magma chamber. As a further simplification the lithospheric density is taken to equal the magma density.

[27] Plate separation is taken to reduce the horizontal stress normal to the dike uniformly with depth in the lithosphere without affecting the vertical stress. Therefore one can write

$$\sigma_h(x,z) = \sigma_v(x,z) + \sigma_d(x), \tag{3}$$

where $\sigma_d(x)$ is the stress difference, assumed here to be depth independent (Figure 8). As a notational simplification we include the effect of variations in surface elevation on the driving pressure in an effective tectonic stress, σ, (hereafter referred to as the tectonic stress) as

$$\sigma(x) = \sigma_d(x) - \rho g z_s(x) = \sigma_h(x,z) - \rho g z. \tag{4}$$

4.2. Dike Opening and Regional Tectonic Stress

[28] Consider a magmatic "event" in which magma from a localized chamber is injected into a dike cutting tectonically stressed lithosphere. An intrusion "event" is the rapid emplacement of a single dike during which the dike and the magma chamber constitute a "closed system".

[29] Intrusion of magma pushes the walls of a dike apart and increases the local value of the minimum principal stress. This means that the tectonic stress increases (i.e., becomes more compressive). The magnitude of stress change when a dike opens depends on properties of the lithosphere and asthenosphere. The asthenosphere is here defined as the region that flows viscously to relieve most elastic stresses building up on the scale of time between diking episodes. The lithosphere does not flow significantly on this timescale. During the short time of a diking event the asthenosphere should act as an elastic layer with nearly lithostatic stress (Figure 6). Thus the asthenosphere can limit how much the lithosphere opens when cut by a dike. Because of the vertical variation in prestress it is not correct to use the equations describing opening of a pressurized crack in an elastic half-space which would predict a quadratic variation of dike width and driving pressure [*Weertman*, 1971]. Numerical experiments simulating dike opening with a reasonable vertical variation of prestress indicates a nearly linear relation between driving pressure and dike width (Ran Qin, personal communication, 2006).

[30] Thus we assume that during dike intrusion the lithosphere behaves as an elastic solid over a horizontal distance scale normal to the dike equal to the height of the dike, H (Figure 6a). Stress changes at a distance from the magma chamber depend only on the dike widening at that position. The lithosphere-asthenosphere system along an opening dike is taken to behave like a series of independent, finite length springs orthogonal to the dike. If the initial tectonic stress is σ^i then the final stress after the dike event is taken to depend linearly on dike opening as

$$\sigma^f(x) = \sigma^i(x) + (\delta\sigma/\delta w) w(x), \tag{5}$$

where $w(x)$ is the width of an intruded dike and $\delta\sigma/\delta w$ is analogous to a "spring constant" for the lithosphere. We expect $\delta\sigma/\delta w \sim E/H$, where E is the Young's Modulus of the lithosphere.

4.3. Magma Withdrawal and Magma Chamber Pressure

[31] Assume that magma pressure P decreases linearly with the volume going into the dikes (see Figure 7). If the initial magma pressure is P^i then after a volume of magma ΔV_{out} is removed from the chamber the final magma pressure is

$$P^f = P^i - (\delta P/\delta V)\Delta V_{out}, \tag{6}$$

where $\delta P/\delta V$ is a constant that depends on the initial volume, shape and depth of the magma chamber, and the rheologic properties of the rock in and around the chamber. This linear relation holds if the surroundings respond in an elastic manner and if strains are small [*Mogi*, 1958]. The larger the magma chamber the smaller should be the value of $\delta P/\delta V$ [*Mogi*, 1958].

4.4. Relations Between Magma Pressure, Tectonic Stress, and Magma Volumes

[32] We assume that during and at the end of a dike intrusion event the magma pressure and the tectonic stress are equal along the length of a dike where magma was intruded:

$$P^f = \sigma^f(x) \quad \text{for} \quad x_1 < x < x_2. \tag{7}$$

We define x_1 as the end of the dike at, or closest to, the magma chamber and x_2 as the far end of the dike (Figure 8).

[33] The depth Δz_d of the top of a dike below the local surface (Figure 8) depends on the final magma pressure and since this equals the final local tectonic stress we can write this as

$$\Delta z_d(x) = \frac{-\sigma^f(x)}{\rho g} - z_s(x). \tag{8}$$

For a plausible value of the tectonic stress after intrusion of -10 MPa and $z_s(x) = 0$ m then $\Delta z_d(x) = 364$ m, taking the density of magma $\rho = 2800$ kg/m^3 and g = 9.8 m/s^2. For Krafla we assume that the lithospheric thickness is 10 km and that the bottom of the dike extends to the bottom of the lithosphere. Thus for moderate tectonic stress levels variations the depth of the dike top should have a small effect on the volume of the dike and we ignore it.

[34] For a constant dike height, H, the volume of intruded magma in a given dike event is

$$\Delta V_{in} = H \int_{x_1}^{x_2} w(x)dx = H(\delta w/\delta\sigma) \int_{x_1}^{x_2} \left[P^f - \sigma^i(x)\right] dx. \tag{9}$$

If there is no extrusion of magma then the volume of magma intruded along a dike equals the volume removed from the magma chamber.

4.5. Stopping Dike Propagation

[35] Viscous pressure loss along the body of the dike may be small as the dike slows, however, viscous resistance to flow of magma into the tip of the dike may be considerable. There also may be resistance to dike propagation due to

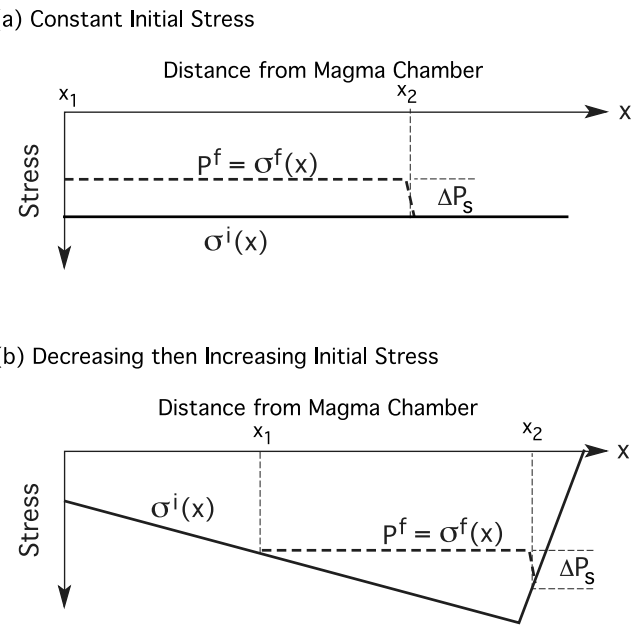

Figure 9. Relation between two initial lithospheric tectonic stress (prestress) distributions and the final stress along a dike and the positions of the dike ends for a single dike intrusion event. (a) For a constant prestress as a function of distance from a magma chamber there is a uniform increase in stress, equal to the minimum driving pressure for propagation, ΔP_S, out to a distance $x = x_2$. Because lithospheric strain is proportional to stress change, the amount of dike opening is predicted to be uniform with distance along the dike. (b) If the tectonic stress decreases over a certain distance and then increases, the dike may be open only beyond a distance $x = x_1$ from the magma chamber.

fracturing of rock around the tip of the dike. We assume that the complex processes at the dike tip combine to so that the velocity of dike tip propagation depends linearly on the driving pressure at the tip ($P^f - \sigma^i(x_1)$).

[36] A certain level of driving pressure in needed for magma to breakout of the magma chamber to initiate a dike and it is designated $\Delta P_B = P^i - \sigma^i(0)$. As a dike propagates and opens the magma pressure is reduced as magma is withdrawn from the chamber. Thus the driving pressure and propagation velocity will be reduced as a dike lengthens. When the driving pressure drops to a certain value the dike should stop, either because it is propagating so slowly that the magma in the tip freezes, or because the dike can no longer overcome static resistance to deformation at the tip. We define ΔP_S as the minimum driving pressure before the dike stops, so a dike will stop when $P^f - \sigma^i(x_2) = \Delta P_S$.

[37] We can derive a simple expression for the reduction in driving pressure with dike length, L, for the case of uniform initial tectonic stress with distance from the magma chamber. Then changes in tectonic stress and so the width of the dike will be constant along its length. The intruded volume ΔV_{in} is HwL where $w = (P^f - \sigma^i)/(\delta\sigma/\delta w)$ by equation (5). If the volume going into the dike equals the volume coming out of the magma chamber than we can use equation (6) to calculate the reduction in magma pressure and so the reduction in driving pressure is

$$P^f - \sigma^i(x) = \frac{\Delta P_B}{\left(1 + {}^{L}\!/_{L_o}\right)}, \tag{10}$$

where L_o is a characteristic length of dike propagation and

$$L_o = (\delta\sigma/\delta w)/H(\delta P/\delta V). \tag{11}$$

If velocity is proportional to driving pressure then equation (10) shows how propagation velocity decreases with dike length and this relation is consistent with the observed slowing of the propagation Krafla dikes [*Einarsson and Brandsdóttir*, 1980].

[38] The minimum driving pressure sets the amount of stress change at the tip of the dike and this is what links the position of the end of the dike and the final tectonic stress (see Figures 8 and 9). Thus the final length of a dike propagating into uniformly stressed lithosphere is equal to L_o (($\Delta P_B/\Delta P_S$) − 1). Clearly a dike can only propagate if the breakout pressure is greater than the stopping pressure. In general dikes will be shorter for larger values of ΔP_S, $|\delta P/\delta V|$ and H, or for smaller values of $\delta\sigma/\delta w$ and ΔP_B.

5. Numerical Simulation of Dike Events

[39] The intrusion of a dike produces changes in the stress field that may change where a second dike may intrude. To illustrate the characteristics of our idealized dike intrusion model we describe a simple numerical scheme to track magma volumes intruded into dikes and associated stress changes for a series of dike events. A grid is set up along the axis of propagation (the *x axis*) with a grid spacing that is a small fraction (<1/100) of the characteristic dike length L_o.

[40] Dikes propagate either in the $+x$ or $-x$ direction, but not in both directions at once. A dike propagates in the direction of the largest local negative gradient of stress with distance from the magma chamber (i.e., the dikes are pulled into the most tensional areas). Different test positions of the far end of the dike, x_2, are tried with the stress everywhere along the dike assumed to be changed to $\sigma^i(x_2) + \Delta P_S$. If this test final stress is greater than the initial stress at the magma chamber then the position x_1 equals zero (i.e., the dike is open at the magma chamber.) If the test stress is less than the initial stress at $x = 0$ then x_1 is set at the position where the initial stress equals the final stress along the dike. We compute the stress changes everywhere along the dike and use equation (5) to calculate the dike width, $w(x)$ along the dike.

[41] The magma volume ΔV_{in} in the test dike is the integral of $w(x)H$ between the start and end of the dike (equation (9)). Assuming this volume is removed from the magma chamber we use equation (6) to estimate the magma pressure resulting from this test dike. If this value of pressure is greater than $\sigma^i(x_2) + \Delta P_S$ then there is excess pressure available to drive the dike to propagate further. Thus we increase x_2 and repeat the test until the final magma pressure is equal to or slightly less than the final stress along the dike. Having set the end of the dike we update stresses along the dike to a value of $\sigma^i(x_2) + \Delta P_S$. At the end of the

dike we taper the stress changes over three points, being careful not to change the volume of intruded magma. There are two reasons for this tapering. First, tapering in dike width is likely to occur in nature. Second, it eliminates some numerical model irregularities as described below.

[42] Applying these rules for different stress distributions gives different predicted distributions of dike opening. For an initially uniform stress distribution the tectonic stress change, and so the width of the dike is uniform along the dike, as shown in Figure 9a. If the stresses decrease (i.e., become more tensile) with distance from the magma chamber then a dike can propagate farther from the magma source. According to our assumptions the dike would first open near the magma chamber, but as the dike continued to propagate the tail of the dike would close. This is much like a horizontally propagating version of a vertically propagating, buoyancy driven "Weertman crack" [*Weertman*, 1971]. It is likely that some magma would have frozen in the tail of the dike before it closed, but we ignore that possibility. Figure 9b illustrates a case where a dike stopped because it ran into an area of increasing stress.

6. Results for Multiple Dike Events

6.1. Constant Initial Stress

[43] To deal with multiple dike intrusion events we must specify stress changes near the magma chamber as well as far from that source region. The tectonic stress at the magma chamber (at $x = 0$) is changed by half the amount of the change in an adjacent point. For example, if a dike propagates in the $+x$ direction into a uniform tectonic stress field, the stresses between $x = 0$ and $x = L$ are increased by ΔP_S, while $\sigma_f(0) = \sigma_i(0) + \Delta P_S/2$. Figure 10a for event 1 illustrates this change in stress and magma pressure for $\Delta P_B = 2\Delta P_S$.

[44] If the breakout pressure, ΔP_B is constant for every dike event then an increase in the tectonic stress at the magma chamber ($x = 0$) results in a higher value of the magma pressure needed for the start of propagation of the next dike. The second dike propagates in the $-$x direction, because tectonic stresses adjacent to the magma chamber are lower in that direction. The second dike propagates farther than the first because the pressure needed for the breakout has increased by $\Delta P_S/2$ (see Figure 10a). After event 2 the stress at the magma chamber is now essentially the same as for adjacent regions.

[45] We assume that there has been infinitesimal lowering of the tectonic stress in the region of the first dike, as might happen because of viscoelastic relaxation, so that a third dike propagates in the $+x$ direction. Because of the tapering of the dike width and associated stress changes near the end of dike number 1 the third dike can "spill" into the region of lower tectonic stresses beyond the end of the first dike. The total length of the third dike is larger than the first two, because of the increased initial magma pressure needed to overcome the higher tectonic stresses at the magma chamber.

[46] The third dike does not affect the stresses along the length of dike 1, except at its tapered end, so the next dike also propagates in the $+x$ direction. This fourth dike propagates exactly like the first dike (see Figure 10a). The fifth dike propagates in the $-x$ direction and like dike 3 it propagates far from the origin and does not affect stresses in the region of dike 2.

[47] As shown for the 20 dike sequence illustrated in Figure 10a, a simple pattern of dike propagation emerges. Dikes propagate in one direction, a relatively large distance from the origin. Subsequent dikes propagate decreasingly great distances from the origin (the model magma chamber location) until a dike relieves some tectonic tension at the origin. The next dike then propagates in the opposite direction with later dikes propagating shorter distances. The magma chamber pressure variations (Figure 10a) show that the longest dikes correspond to the largest pressure drop. Also, the magma pressure at breakout increases when the tectonic stress at the origin increases (i.e., becomes more compressive). Recall that this occurs because the pressure to breakout of the model magma chamber is set to be a constant value ($=\Delta P_B$) above the local tectonic stress. The model of evolving stresses depends only on three parameters: ΔP_B, ΔP_S and L_0. If we assume greater magma pressures at breakout, this leads to longer dikes, but the pattern of diking is similar to that for the smaller value of ΔP_B.

6.2. Distribution of Steady State Stress or Topography

[48] Stresses in an extensional region affected by dikes emanating from a magma chamber should evolve in a series of dike intrusion episodes that increase tectonic stresses followed by periods of tectonic extension that lowers tectonic stress. If the episodes did not lead to either extrusion of lava in some areas or normal faulting in others then the pattern of dike stress changes (and associated extensional straining) could be similar to that shown in Figure 10. However, it is likely that dike episodes result in extrusion in some areas and faulting in others. Such activity would result in along-axis topography.

[49] Dike episodes might end with extrusion when all tectonic stress differences are relieved. Extrusion would first occur and build topography near the magma chamber. As elevations increase near $x = 0$ there would be a topographic stress gradient favoring extrusion at the edge of the extrusive topography.

[50] Far from the magma chamber tectonic stresses might be sufficient for normal faulting. Fault-related lowering of topography eventually would drive dikes to extrude for large x. Extrusion for $x > 0$. can only happen if the topographic gradient is sufficient to offset the reduction in magma pressure as a dike propagates laterally.

[51] An equilibrium topographic profile along a segment axis is one where extrusion during a dike event could happen at all distances from the magma chamber. This equilibrium topographic relief depends on the tectonic stress distribution divided by density contrast times gravitational acceleration, ρg. Simple analysis shows that the stable topography with distance from the center of a model segment depends mainly on the characteristic propagation length L_0. The predicted slope depends in the inverse square root of L_0. If L_0 is small then the slope is large. L_0 is sensitive to the magma chamber properties. For a large magma chamber we expect that $\delta P/\delta V$ will be small and so L_0 will be large. Thus a ridge with a small magma chamber should have a large equilibrium slope.

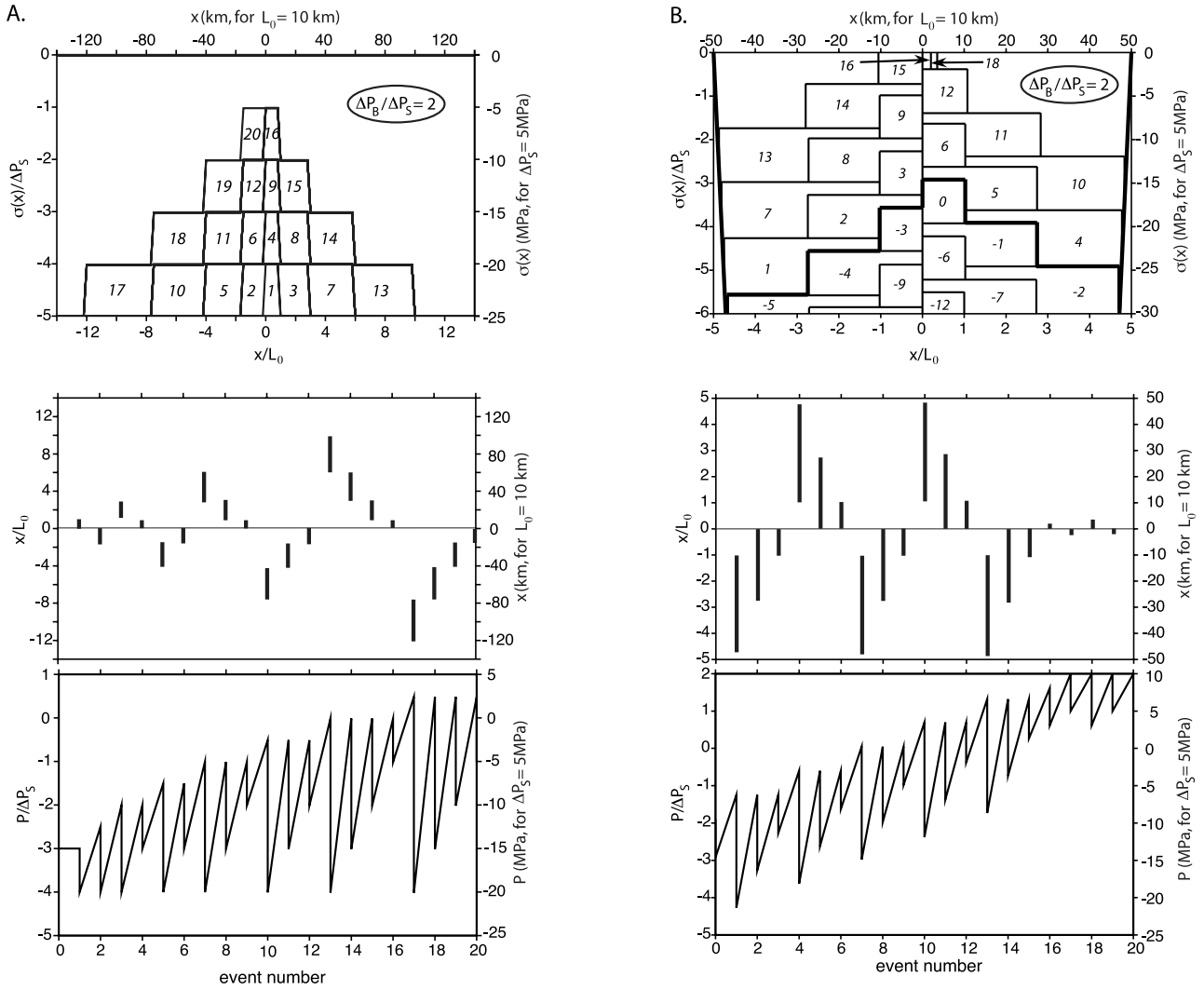

Figure 10. Model results for 20 dike intrusion events with the excess breakout magma chamber pressure for each event, ΔP_B, equal to twice the stopping pressure ΔP_S. (a) Results for a uniform initial prestress. (top) Tectonic stress, divided by ΔP_S, at the end of each event, with the event number printed next to the corresponding stress plot. The horizontal distance from the magma chamber, x, is divided by the characteristic length for dike propagation, L_0. (middle) Horizontal distance range for dike opening for each event. (bottom) Magma pressure changes for each event. (b) Same as Figure 10a except with prestress barriers at a set distance from the magma chamber. The stress barriers are places where the tectonic stress increases markedly to a level that prevents dike propagation. Here we show the last 20 events of a sequence of 100 events. The pattern of events becomes repetitious until tectonic stresses approach zero and magma pressure may be greater than zero, which is assumed to lead to extrusion and so little propagation of dikes.

6.3. Constant Initial Stress and Stress Barriers

[52] A mid-ocean ridge volcano tectonic system does not exist in isolation. The stress fields of adjacent systems will affect each other. Also, transform faults may separate ridge segments fed by different volcanic systems. The transforms may be places across which tectonic stresses change and may even be compressive. A dike should not propagate into these adjacent areas of higher (i.e., more compressive) stresses.

[53] To illustrate the effect of stress "barriers," or areas of appreciably more relative tectonic compression, on the pattern of dike propagation in our model we carried out the following model experiment. We started with uniform negative (i.e., relatively tensile) stresses out to a distance of 5 L_0 in each direction where the stress abruptly increases to lithostatic (i.e., $\sigma(\pm 5L_0) = 0$). The introduction of this length scale means that dikes cannot propagate farther than 5 L_0 from the origin and the number of dikes that occur sequentially in one direction is limited. In this case no more than three dikes propagate in the same direction before a dike breaks out in the opposite direction. Figure 10b illustrates the last 20 dikes in a sequence of 50 dikes that began with a uniform tectonic stress of -20 MPa between $x = -5L_0$ and $x = +5L_0$. A very regular pattern of dike

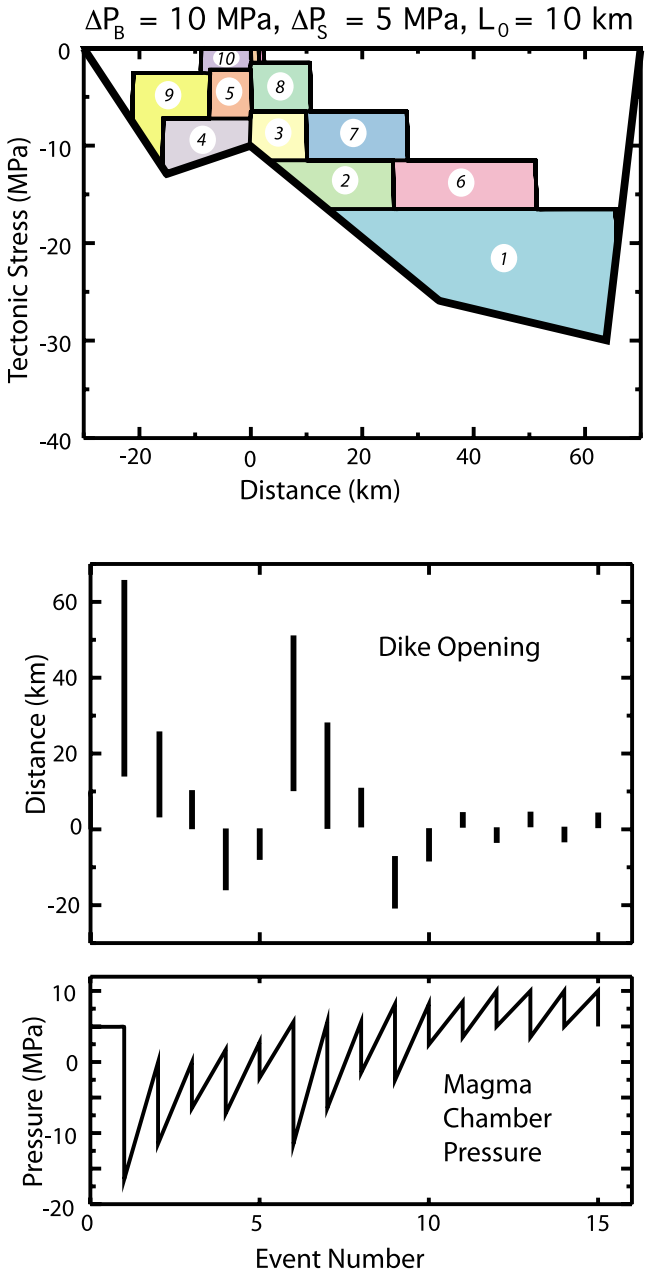

Figure 11. Model results for 15 events with an initial stress pattern approximating possible conditions for the Krafla episode. Here the characteristic length for dike propagation, L_0, is 10 km, and the first event has an excess breakout pressure ΔP_B of 25 MPa (5 times ΔP_S = 5 MPa), while for all other events $\Delta P_B = 2\Delta P_S$ = 10 MPa. Note the broad similarity of the results to the data shown in Figure 2.

propagation results with three dikes going in the $+x$ direction. Unlike the previous simple model experiment, the introduction of a length scale into the stress field results in a steady increase in the lowest magma pressure during a dike intrusion event.

[54] As the tectonic tension is reduced in the vicinity of the model magma chamber the magma pressure at breakout may be greater than zero. In other words the magma pressure is large enough to drive extrusion of magma.

6.4. Magma Extrusion

[55] When magma pressure at the surface of an open dike is positive then extrusion can occur. This means that the horizontal principal stress is equal to or greater than the vertical stress. Give our formulation this will happen when magma pressure is greater than $-\rho g z_s(x_2)$. When extrusion occurs the excess magma pressure above the surface pressure will drive extrusive flow and less magma pressure will be available to drive dike propagation. Whether dikes continue to propagate or stop once extrusion begins should depend on the tectonic stress ahead of the dike tip. We assume that the magma pressure will drop to the local surface pressure at the start of extrusion ($= -\rho g z_s$). The dike will continue to propagate after the start of extrusion if

$$-\rho g z_s(x_2) - \sigma(x_{2+}) > \Delta P_S, \tag{12}$$

where the subscript "+" added to x_2 implies a position just ahead of the tip where stresses have not been affected by the dike opening. Since the present treatment does not deal with viscous pressure changes and the rate of propagation of the dike we cannot estimate magma extrusion as the dike continues to propagate. We ignore extrusion in cases when propagation continues to the point where extrusion ceases.

[56] If the dike does continue to propagate, extrusion will cease if the magma pressure everywhere drops below the surface pressure, like in the events of 20 December 1975, 29 April 1977, 8 September 1977 and 16 March 1980. If condition (12) is not met then the extrusion should continue until enough magma is drained from the magma chamber so that the magma pressure drops to the surface pressure, like for eruption events after March 1980. This allows us to estimate the volumes of eruptions in events where dike propagation stops and extrusion continues.

[57] For the model experiment illustrated in Figure 10b the last few events imply extrusion with no further dike propagation because the magma pressure at dike breakout is greater than the surface pressure near the magma chamber. Large volumes of magma may be extruded because the pressure available to drive extrusion is large.

6.5. A Krafla Rifting Episode Model

[58] Our idealized model naturally produces sequences of decreasing length dikes and alternation of the direction of propagation for each sequence. Also, the model implies that large extrusive events may occur the end of an episode of dike events when most of the relative lithospheric tension has been relieved by dike intrusion. This matches the primary characteristics of the sequence of events in the Krafla sequence.

[59] There are several reasons to construct a model setup specifically aimed at the Krafla episode. The Krafla episode is marked by asymmetry, with longer dikes propagating to the north than to the south. Also, other observations, such as widening of the fissure swarm and subsidence above the magma chamber during each dike event, can be used to constrain model parameters. To see whether a reasonable initial tectonic stress field can lead to a pattern of dikes that is closer to that observed for the Krafla episode we set up the model illustrated in Figure 11. The assumed effective stress variations are based on a simplified topographic profile (see Figure 4) using a rock density of 2800 kg/m^3

in equation (4). There is a stress barrier at 70 km to the north (+x direction) of the magma chamber, which represents a transform boundary. To the south (the $-x$ direction) there is a gradual an increase in tectonic stress that plausibly might be related to the relief of relative tension in the Askja volcano tectonic events of 1874–1876 [*Sigurdsson and Sparks*, 1978; *Brandsdóttir*, 1993]. The effective tectonic stresses are set to be −10 MPa at the origin (at the magma chamber) and this is meant to represent stresses produced by plate separation since the last dike intrusion episode.

[60] The other model parameters are set as follows: the brittle layer thickness H = 10 km, $\delta\sigma/\delta w$ = 3 MPa/m, the breakout pressure ΔP_B = 10 MPa, the minimum driving pressure ΔP_S = 5 MPa, and the ratio of magma pressure change to volume withdrawn from the chamber $\delta P/\delta V = 3 \times 10^{-2}$ Pa/m^3 (= 30 MPa/km^3). Thus by equation (11), L_0 = 10 km.

[61] The first event could not be treated the same way as the subsequent events. The first dike event had the greatest length and width, and had by far the longest time of opening. It propagated to the intersection of the fissure swarm and the Grímsey oblique rift, beyond which the stress is likely not sufficient to allow propagation. The magnitude of the opening requires that at least one of the model parameters is different for this event than for the subsequent events. In the simulation illustrated in Figure 10 the first event has a breakout pressure that is 2.5 times larger than for the later events. It is plausible that the breakout of the first event is more difficult than the later events, since the first dike may leave a hot, weak slot near the magma chamber that could aid formation of the later events.

[62] The simulation reproduces the main pattern of dikes for 10 out of the first 11 larger events: three dikes to the north, two to the south, three to the north and two to south. Compare Figures 2 and 11. The transition to extrusion and no more propagation is consistent with observations after the second northern sequence. The model does not predict smaller events. The amount of widening of the fissure swarm (given by the stress change on Figure 10 divided by $\delta\sigma/\delta w$ = 3 MPa/m) is under predicted by a factor of 2. The predicted amount of widening is fairly uniform along the segment, while geodetic estimates indicate more widening close to the caldera [*Tryggvason*, 1984].

[63] The amount of elevation change over the magma chamber is estimated using a Mogi model [*Mogi*, 1958] for the effect of magma withdrawal as shown on Figure 11. The results are very close to that observed (Figure 2) if the Young's Modulus of the rock is 3×10^{10} Pa and if the depth magma chamber is 3 km. The magma chamber depth is constrained seismically [e.g., *Einarsson*, 1978; *Brandsdóttir and Menke*, 1992; *Brandsdóttir et al.*, 1997] and geodetically [e.g., *Björnsson et al.*, 1979; *Ewart et al.*, 1991].

6.6. Variables and Constraints

[64] We do not formally invert for parameters in this model since we neglect processes, like the viscoelastic relaxation of the lithosphere, that likely affect the pattern of dike opening during an episode. It appears that the observations do constrain model variables to about a factor of 2. Some variables are directly constrained, such as the thickness of the brittle lithosphere. Since seismicity is observed down to 10 km this should be close to the thickness, H, of the brittle lithosphere. Laboratory measurements on the elastic moduli of basalts constrains the change in tectonic stress with dike widening since, as argued earlier $\delta\sigma/\delta w \sim E/H$, where E is the Young's modulus. For $E = 3 \times 10^{10}$ Pa this means that $\delta\sigma/\delta w$ = 3 MPa/m. This leaves four parameters of the model to be constrained by the observations of the dike intrusion sequence. These are the pressure-volume relation for the magma chamber, $\delta P/\delta V$, the breakout driving pressure, ΔP_B, the minimum driving pressure for dike propagation, ΔP_S, and the stress distribution.

[65] There are five observation types for the Krafla episode that constrain these four variables. (1) The characteristic width of opening should be given by $\Delta P_S/(\delta\sigma/\delta w)$. It is observed to be a bit more than 1 meter. Using ΔP_S = 5 MPa and the value of $\delta\sigma/\delta w$ given above we get a typical maximum dike width of 1.67 m. (2) The fact that at least two dikes open above the magma chamber before there is a major eruption indicates that the initial stress at the origin $\sigma_0(0) \sim 2\Delta P_S \sim 10$ MPa. (3) Because some small eruptions occur while dikes still propagate suggests that $\Delta P_B \sim \sigma_0(0) \sim 10$ MPa. (4) The characteristic dike propagation length: $((\Delta P_B/\Delta P_S) - 1)L_0 \sim L_0$ has to be close to 10 km to give the right range of dike lengths in the episode. Given the definition of L_0 then $\delta P/\delta V \sim (\delta\sigma/\delta w)/h\ L_0 \sim 30$ MPa/km^3. Note that this is similar to the value of pressure volume relation estimated for the Kilauea Volcano magma chamber by *Denlinger* [1997]. (5) Finally, the subsidence of the surface above the magma chamber acts as a check on our estimated magma volume for each dike event. The volume intruded depends on width, length, and height of the dike. The length and height of the dike is estimated from seismicity and the width is constrained by geodetics. Caldera subsidence depends on the volume of magma taken from the chamber and on the depth of the magma chamber.

[66] Neglecting viscoelastic relaxation may have a significant effect on the model dike widening, but may not fundamentally alter the pattern of propagation. The ~5 month average time between the major propagating events should limit the amount of viscoelastic stress relaxation between events to several tens of percent of the syn-dike stress change [e.g., *Foulger et al.*, 1992].

7. Discussion

[67] The basic idea of this model is that dike propagation is controlled by tectonic stress and magma pressure. The magma pressure is reduced as volume is extracted from a magma chamber. The dike stops propagating when the "driving pressure" (defined as the difference between magma pressure and tectonic stress orthogonal to the dike) becomes too small, either because the dike slows and the tip freezes or because the driving pressure is not enough to break open a new section of dike. The system naturally oscillates with a sequence of decreasing length dikes propagating in one direction followed by another sequence in the opposite direction. Major eruptions can occur only after most of the tectonic stress is relieved by dike opening. The model gives a reasonably good fit to the observed features of the Krafla dike intrusion episode, even though many factors that likely affect diking are neglected. The point of the direct comparison to the Krafla episode data is to show that a simple model predicts the sequential development and

magnitude of opening of a series of dikes on one well-studied segment of a mid-ocean ridge.

7.1. Applications to Other Settings

[68] As mentioned above, the two previous rifting episodes in the northern rift zone, those of Krafla 1724–1729 and Askja 1874–1876 served as predictive models for the development of the Krafla 1975–1984 episode. The change from mostly intrusive activity in the beginning of the episode to mostly eruptive activity toward the end that is reproduced by our model. The limited data we have for these earlier episodes are also consistent with other predictions of our model, i.e that the activity in the beginning is spread along considerable part of the fissure swarm and converges later toward the central volcano as it becomes more eruptive.

[69] The gigantic Laki eruption 1783 (when $\sim$15 km^3 of lava extruded) and associated dike activity also conforms with aspects of our model. The activity of the Laki fissure can be divided into 10 episodes, each one occurring on a segment closer to Grímsvötn, a central volcano northeast of the Laki fissures [*Thordarson and Self*, 1993]. The fissure eruptions were then followed by four eruptive episodes in the subglacial Grímsvötn volcano until the end of the activity in 1785 [*Thordarson*, 2003]. Some workers suggest that the source of the magma for the eruptions were from the southwest of the fissures and that the sequence involved legthening dikes. However, our model is consistent with the notion that the Laki-Grímsvötn activity was fed from the Grímsvötn volcano, as was suggested by *Sigurdsson and Sparks* [1978]. The magma pressures were greater and the chamber refilling time was much shorter than for the Krafla episode.

[70] *Takada* [1997] shows that several other volcanoes show patterns of dike propagation distance and direction changes that are similar to those seen in the Krafla episode. It is encouraging that the Krafla pattern is not unique and it is worthwhile to consider the causes for the differences in the patterrns of dike propagation episodes that Takada has noted.

[71] There is evidence of central magma chambers supplying magma to most slow and some intermediate spreading rate ridge segments. For example, most of the 40–150 km long segments of the slow-spreading mid-Atlantic Ridge axial depths increase with distance from segment center with as much as 2 kilometers of relief [e.g., *Lin et al.*, 1990]. Gravity and seismic data are consistent with a decrease in the average thickness of the igneous crust with distance from the segment center [e.g., *Lin et al.*, 1990; *Tolstoy et al.*, 1993]. Seismic tomography also indicates the very lowest seismic velocities at segment centers [*Magde et al.*, 2000]. At ultraslow-spreading ridges, defined as ridges with effective spreading rates less than 1.2 cm/yr there are indications that ends of segments may have no magmatic crust while the segment center is marked by volcanic constructs [*Dick et al.*, 2003]. These observations may be consistent with our model if the central magma chamber becomes smaller with decreasing spreading rate. Then the characteristic length of dike propagation should decrease and the equilibrium along-axis topographic slope increase with slower spreading rates. For ultraslow-spreading ridges the maximum length of dike propagation might be less than the half-segment length, leading to regions never intruded by a dike.

[72] Fast-spreading ridges have the smallest along-axis topographic relief, as low as 0.1 m per kilometer [*Wang and Cochran*, 1993], but it is not clear whether fast-spreading segments are largely fed by magma from a central magma chamber. Ridge morphology, lava flow style and magma chemistry may indicate central supply [e.g., *MacDonald*, 1998], however, magma lens are imaged seismically along most fast-spreading segments [e.g., *Hooft et al.*, 1997].

7.2. Does Large Magma Flux Allow Long Dikes?

[73] If magma pressure reduction due to extraction of magma from a chamber is as important as the Krafla data suggests then very large magma chambers could lead to very long distance propagation of dikes. The larger a magma chamber the smaller the pressure reduction on extraction of a unit volume of magma [*Mogi*, 1958]. Simple thermal arguments would suggest that the size of a magma chamber should correlate with the flux of magma coming into a region. Magma flux into a ridge segment should scale with spreading rate, possibly explaining the spreading rate dependence of along-axis crustal and topographic relief noted above.

[74] The greatest known fluxes of magma occur during the geologically short periods when large igneous provinces such as the Deccan Traps or the Parana basalts form. The volumes are up to several million cubic kilometers and the time interval of high-rate magma output is 1 m.y. or less [*Courtillot and Renne*, 2003]. We speculate that very large magma chambers are likely to form during periods of high rate and localized melt flux. Magma chambers the size of large gabbroic layered intrusions found near the centers of some large igneous provinces could feed dikes propagating thousands of kilometers. For example, the Skaergaard layered intrusion of East Greenland is estimated to have a volume of $\sim$300 km^3 [*Nielsen*, 2004], sufficient to fill a dike 2000 km long, 50 km high and 3 m thick. *Buck* [2004] points out that dike intrusion on a massive scale could promote rifting of normal continental lithosphere, but only if there were considerable tectonic extensional stress available to drive the intrusion and propagation of those dikes. The nearly linear structure of most "volcanic rifted margins", like the Red Sea, East Greenland or the eastern margin of South America [e.g., *White and McKenzie*, 1989] argue for gigantic dikes fed from very large magma chambers.

7.3. Future Work

[75] Our model does not include time- and rate-dependent processes, such as viscous pressure changes between the magma chamber and the dike tip region. In future versions of our model we intend to include viscous pressure changes in the body of the dike, which must be estimated if we are to determine the time progression of individual dikes or predict eruption during dike propagation events [e.g., *Pinel and Jaupart*, 2004].

[76] The time evolution of dike events on a magmatic segment may be affected by viscoelastic relaxation of the lithosphere/asthenosphere. On the interevent timescale (months to years) there is considerable "recharging" of the lithospheric stress by relaxation of the underlying

viscous asthenosphere. Another critical process is the refilling of the magma chamber, which is likely affected by melt migration through a porous matrix and viscous flow of that matrix. Finally, a time-dependent model might include cooling of dikes near the chamber, since this may affect the breakout pressure needed to initiate a dike. Clearly these models require a different order of complexity than the present simple approach.

Notation

Defined Parameters

- x horizontal distance along axis from magma source.
- y horizontal distance across axis from dike center.
- z vertical distance below land surface at magma source.
- $P_m(z)$ magma pressure.
- $\sigma_h(x,z)$ horizontal stress normal to dike.
- ρ density of magma or crust.
- g acceleration of gravity.
- P magma pressure reduced by ρgz.
- $\sigma(x)$ horizontal stress normal to dike reduced by ρgz.
- x_1 position of dike end closest to source.
- x_2 position of dike end farthest to source.
- $z_s(x)$ depth of surface below surface at source.
- $\Delta z_d(x)$ depth of dike below local surface.
- $w(x)$ dike thickness.
- L length of dike opening ($= x_2 - x_1$).
- ΔV volume of magma out of chamber or into dike.

Model Variables

- H height of dike = lithospheric thickness.
- $\delta P/\delta V$ pressure-volume factor for magma source.
- $\delta\sigma/\delta w$ tectonic stress-widening factor for dike.
- ΔP_B driving pressure for source breakout.
- ΔP_S driving pressure when dike stops.
- L_o characteristic dike length [$= (\delta\sigma/\delta w)/H(\delta P/\delta V)$].

[77] **Acknowledgments.** We dedicate this work to Ármann Pétursson, a farmer in Reynihlíd who monitored and serviced the analog seismic stations and tiltmeters in the Krafla region throughout the rifting episode. Thanks to Bill Menke and Ran Qin for helpful discussions and three anonymous reviewers for comments that improved the paper. W.R.B. supported by NSF grants OCE 0242597 and OCE 0426575 LDEO contribution 6987.

References

Björnsson, A., K. Saemundsson, P. Einarsson, E. Tryggvason, and K. Gronvald (1977), Current rifting episode in North Iceland, *Nature*, *266*, 318–323.

Björnsson, A., G. Johnsen, S. Sigurdsson, G. Thorbergsson, and E. Tryggvason (1979), Rifting of the plate boundary in North Iceland 1975–1978, *J. Geophys. Res.*, *84*, 3029–3038.

Brandsdóttir, B. (1993), Historical accounts of earthquakes associated with eruptive activity in the Askja volcanic system, *Jökull*, 1–12.

Brandsdóttir, B., and P. Einarsson (1979), Seismic activity associated with the September 1977 deflation of Krafla Volcano in north eastern Iceland, *J. Volcanol. Geotherm. Res.*, *6*, 197–212.

Brandsdóttir, B., and W. H. Menke (1992), Thin, low-velocity zone within the Krafla caldera, NE-Iceland, attributed to a small magma chamber, *Geophys. Res. Lett.*, *19*, 2381–2384.

Brandsdóttir, B., W. Menke, P. Einarsson, R. S. White, and R. K. Staples (1997), Faeroe-Iceland Ridge Experiment: 2. Crustal structure of the Kafla central volcano, *J. Geophys. Res.*, *102*, 7867–7886.

Bruce, P. M., and H. E. Huppert (1990), Solidification and melting along dikes by the laminar flow of basaltic magma, in *Magma Transport and Storage*, edited by M. P. Ryan, pp. 87–101, John Wiley, Hoboken, N. J.

Buck, W. R. (2004), Consequences of asthenospheric variability on continental rifting, in *Rheology and Deformation of the Lithosphere at Continental Margins*, edited by G. D. Karner, B. Taylor, N. W. Driscoll and D. L. Kohlstedt, pp. 1–31, Columbia Univ. Press, New York.

Courtillot, V. E., and P. R. Renne (2003), On the ages of flood basalt events, in *The Earth's Dynamics*, edited by V. E. Courtillot, *C. R. Geosci.*, *335*, 113–140.

Delaney, J. R., D. S. Kelley, M. Lilley, D. A. Butterfield, J. A. Baross, W. S. D. Wilcock, R. W. Embley, and M. Summit (1998), The quantum event of oceanic crustal accretion: Impacts of diking at mid-ocean ridges, *Science*, *281*(5347), 222–230.

Delaney, P. T., and D. D. Pollard (1982), Solidification of basaltic magma during flow in a dike, *Am. J. Sci.*, *282*, 856–885.

Denlinger, R. P. (1997), A dynamic balance between magma supply and eruption volume at Kilauea Volcano, Hawaii, *J. Geophys. Res.*, *102*, 18,091–18,100.

Dick, H. J. B., J. Lin, and H. Schouten (2003), An ultraslow-spreading class of ocean ridge, *Nature*, *426*, 405–412.

Dziak, R. P., C. G. Fox, and A. E. Schreiner (1995), The June–July 1993 seismo-acoustic event at CoAxial segment, Juan de Fuca Ridge: Evidence for a lateral dike injection, *Geophys. Res. Lett.*, *22*, 135–138.

Einarsson, P. (1978), *S*-wave shadows in the Krafla caldera in NE-Iceland, evidence for a magma chamber in the crust, *Bull. Volcanol.*, *41*, 1–9.

Einarsson, P. (1986), Seismicity along the eastern margin of the North American Plate, in *The Geology of North America,* vol. M, *The Western North Atlantic Region: Geological Society of America*, edited by P. R. Vogt and B. E. Tucholke, pp. 99–116, Geol. Soc. of Am., Boulder, Colo.

Einarsson, P. (1991), The Krafla rifting episode 1975–1989, in *Náttúra Mývatns* (*The Nature of Lake Mývatn*), edited by A. Gardarsson, and Á. Einarsson. pp. 97–139, *Icelandic Nature Sci. Soc.*, Reykjavík.

Einarsson, P., and B. Brandsdóttir (1980), Seismological evidence for lateral magma intrusion during the July 1978 deflation of the Krafla volcano in NE-Iceland, *J. Geophys.*, *47*, 160–165.

Einarsson, P., and K. Saemundsson (1987), Earthquake epicenters 1982–1985 and volcanic systems in Iceland: A map, in *Í hlutarins eðli, Festschrift for Þorbjörn Sigurgeirsson*, edited by T. Sigfússon, Menningarsjóður, Reykjavík.

Embley, R. W., W. W. Chadwick Jr., I. R. Jonasson, D. A. Butterfield, and E. T. Baker (1995), Initial results of a rapid response to the 1993 CoAxial event: Relationships between hydrothermal and volcanic processes, *Geophys. Res. Lett.*, *22*(2), 143–146.

Ewart, A., B. Voight, and A. Björnsson (1991), Elastic deformation models of Krafla Volcano, Iceland, for the decade 1975 through 1985, *Bull. Volcanol.*, *53*, 436–459.

Fialko, Y. A., and A. M. Rubin (1998), Thermodynamics of lateral dike propagation: Implications for crustal accretion at slow spreading mid-ocean ridges, *J. Geophys. Res.*, *103*, 2501–2514.

Fialko, Y. A., and A. M. Rubin (1999), Thermal and mechanical aspects of magma emplacement in giant dike swarms, *J. Geophys. Res.*, *104*(B10), 23,033–23,049.

Foulger, G. R., C.-H. Jahn, G. Seeber, P. Einarsson, B. R. Julian, and K. Hicki (1992), Post-rifting stress relaxation at the divergent plate late boundary in northeast Iceland, *Nature*, *358*, 488–490.

Gudmundsson, A. (1995), Infrastructure and mechanics of volcanic systems in Iceland, *J. Volcanol. Geotherm. Res.*, *64*, 1–22.

Hirth, G., J. Escartin, J. Lin (1998), The rheology of the lower oceanic crust: Implications for lithospheric deformation at mid-ocean ridges, in *Faulting and Magmatism at Mid-Ocean Ridges*, *Geophys. Monogr. Ser.*, vol. 106, edited by W. R. Buck et al., pp. 291–303, AGU, Washington, D. C.

Hooft, E. E. E., R. S. Detrick, and G. M. Kent (1997), Seismic structure and indicators of magma budget along the southern East Pacific Rise, *J. Geophys. Res.*, *102*, 27,319–27,340.

Ida, Y. (1999), Effects of the crustal stress on the growth of dikes: Conditions of intrusion and extrusion of magma, *J. Geophys. Res.*, *104*(B8), 17,897–17,910.

Karson, J. A. (1998), Internal structure of oceanic lithosphere: A perspective from tectonic windows, in *Faulting and Magmatism at Mid-Ocean Ridges*, *Geophys. Monogr. Ser.*, vol. 106, edited by W. R. Buck et al., pp. 177–218, AGU, Washington, D. C.

Larsen, G. (1984), Recent volcanic history of the Veidivötn fissure swarm, southern Iceland: An approach to volcanic risk assessment, *J. Volcanol. Geotherm. Res.*, *22*, 33–58.

Larsen, G., K. Grönvold, and S. Thorarinsson (1979), Volcanic eruption through a geothermal borehole at Namafjall, Iceland, *Nature*, *278*, 707–710.

Lin, J., G. M. Purdy, H. Schouten, J.-C. Sempere, and C. Zervas (1990), Evidence from gravity data for focused magmatic accretion along the mid-Atlantic Ridge, *Nature*, *344*, 627–632.

Lister, J. R. (1994), The solidification of buoyancy-driven flow in a flexible-walled channel, part 2: Continual release, *J. Fluid Mech.*, *272*, 45–65.

Lister, J. R., and R. C. Kerr (1991), Fluid-mechanical models of crack propagation and their application to magma transport in dykes, *J. Geophys. Res.*, *96*, 10,049–10,077.

Macdonald, K. C. (1998), Linkages between faulting, volcanism, hydrothermal activity and segmentation on fast spreading centers, in *Faulting and Magmatism at Mid-Ocean Ridges*, *Geophys. Monogr. Ser.*, vol. 106, edited by W. R. Buck et al., pp. 27–58, AGU, Washington, D. C.

Magde, L. S., A. H. Barclay, D. R. Toomey, R. S. Detrick, and J. A. Collins (2000), Crustal magma plumbing within a segment of the mid-Atlantic Ridge, 35°N, *Earth Planet. Sci. Lett.*, *175*, 55–67.

Mogi, K. (1958), Relation between the eruptions of various volcanoes and the deformations of the ground surfaces around them, *Bull. Earth. Res. Inst.*, *36*, 99–134.

Nielsen, T. F. D. (2004), The shape and volume of the Skaergaard Intrusion, Greenland; implications for mass balance and bulk composition, *J. Petrol.*, *45*(3), 507–530.

Pinel, V., and C. Jaupart (2004), Magma storage and horizontal dyke injection beneath a volcanic edifice, *Earth Planet. Sci. Lett.*, *221*, 245–262.

Rubin, A. M. (1993), On the thermal viability of dikes leaving magma chambers, *Geophys. Res. Lett.*, *20*, 257–260.

Rubin, A. M. (1995), Propagation of magma-filled cracks, *Annu. Rev. Earth. Planet. Sci.*, *23*, 287–336.

Saemundsson, K. (1974), Evolution of the axial rifting zone in northern Iceland and the Tjörnes Fracture Zone, *Geol. Soc. Am. Bull.*, *85*, 495–504.

Saemundsson, K. (1979), Fissure swarms and central volcanoes of the neovolcanic zones of Iceland, *Geol. J.*, *19*, 415–432.

Segall, P., P. Cervelli, S. Owen, M. Lisowski, and A. Miklus (2001), Constraints on dike propagation from continuous GPS measurements, *J. Geophys. Res.*, *106*, 19,301–19,318.

Sigmundsson, F., H. Vadon, and D. Massonet (1997), Readjustment of the Krafla spreading segment to crustal rifting measured by satellite radar interferometry, *Geophys. Res. Lett.*, *24*, 1843–1846.

Sigurdsson, H., and R. S. S. Sparks (1978), Lateral flow of magma in rifted Icelandic crust, *Nature*, *274*, 126–130.

Sigurdsson, O. (1980), Surface deformation of the Krafla fissure swarm in two rifting events, *J. Geophys.*, *47*, 154–159.

Takada, A. (1997), Cyclic flank-vent and central-vent eruption patterns, *Bull. Volcanol.*, *58*, 539–556.

Thordarson, T. (2003), Laki-Grimsvötn eruptions II: Appraisal based on contemporary accounts, *Jökull*, *53*, 11–48.

Thordarson, T., and S. Self (1993), The Laki (Skaftar Fires) and Grimsvötn eruptions in 1783–1785, *Bull. Volcanol.*, *55*, 233–263.

Tolstoy, M., A. J. Harding, and J. A. Orcutt (1993), Crustal thickness on the mid-Atlantic Ridge: Bull's-eye gravity anomalies and focused accretion, *Science*, *262*, 726–729.

Tryggvason, E. (1980), Subsidence events in the Krafla area, North Iceland, 1975–1979, *J. Geophys.*, *47*, 141–153.

Tryggvason, E. (1984), Widening of the Krafla fissure swarm during the 1975–1981 Volcano-tectonic Episode, *Bull. Volcanol.*, *47*(1), 47–69.

Tryggvason, E. (1994), Surface deformation at the Krafla volcano, North Iceland, 1982–1992, *Bull. Volcanol.*, *56*, 98–107.

Turcotte, D., and G. Schubert (2002), *Geodynamic*, p. 456, Cambridge Univ. Press, New York.

Wang, X., and J. R. Cochran (1993), Gravity anomalies, isostasy and mantle flow at the East Pacific Rise crest, *J. Geophys. Res.*, *98*, 19,505–19,531.

Weertman, J. (1971), Theory of water-filled crevasses in glaciers applied to vertical magma transport beneath oceanic ridges, *J. Geophys. Res.*, *76*, 1171–1183.

White, R. S., and D. McKenzie (1989), Magmatism at rift zones: The generation of volcanic continental margins and flood basalts, *J. Geophys. Res.*, *94*, 7685–7729.

B. Brandsdóttir and P. Einarsson, Institute of Earth Sciences, University of Iceland, Öskju, Sturlugötu 7, IS-101 Reykjavík, Iceland.

W. R. Buck, Lamont-Doherty Earth Observatory, Columbia University, Palisades, NY 10964, USA. (buck@ldeo.columbia.edu)